

Microcalorimetric Study of Nematic-to-Neat-Soap and Nematic-to-Isotropic Phase Transitions in a Lyotropic Liquid Crystal

S. T. Shin and Satyendra Kumar

Department of Physics and Liquid Crystal Institute, Kent State University, Kent, Ohio 44242

(Received 24 September 1990)

The results of specific-heat measurements at the nematic- (N) to-neat-soap (NS) and nematic-to-isotropic (I) phase transitions in binary mixtures of cesium-perfluoro-octanoate and water are reported. The ratio of specific-heat amplitudes above and below the N-NS transition, A^+/A^- , and the specific-heat exponent α remain ~ 1.0 and ≤ 0.02 , respectively, suggesting 3D XY-type behavior. At the first-order N-I transition, the vanishing latent heat and coexistence range at low concentration indicate the existence of a Landau point.

PACS numbers: 64.70.Md, 64.60.Fr, 82.60.Fa

In the binary mixtures of cesium-perfluoro-octanoate (CsPFO) and water, one of the simplest of lyotropics, disklike micelles are formed over a wide range of concentration and temperature. These micelles become orientationally and positionally ordered in one direction, without any appreciable change in their shape and size,¹ forming nematic (N) and neat-soap (NS) phases, respectively. Boden *et al.*¹ found this transition to change from second order to first order as the concentration was raised above ~ 4.58 mole% [later revised to 2.71 mole% (Ref. 1)] of CsPFO. The structural symmetry of the resulting phases and the phase diagrams of this (and similar other) lyotropic system bear striking resemblance to the conventional thermotropic liquid crystals with N and smectic-*A* phases. The N-NS transition has previously been shown^{2,3} to be quite analogous to the N-smectic-*A* transition. Magnetic-birefringence and light-scattering studies² of this system revealed that the nature of the N-I transition also changed from first order in concentrated solutions to nearly second order in dilute solutions. In view of these results, we conducted experiments to study the evolution of specific heat at the two transitions for seven different concentrations.

Calorimetric measurements on these materials are particularly difficult because of the small changes in specific heat (C_p) involved, and the difficulty in handling and sealing these soaplike materials. In a high-resolution ac heat-capacity experiment, Imaizumi and Garland⁴ found the peak C_p values to be only 2% of the background, which is 2 orders of magnitude smaller than in thermotropic materials, for example, 8OCB.⁵ We used a scanning microcalorimeter specially designed for liquid samples. The sample and reference cells of this calorimeter have a capacity of approximately 1.2 ml and are made of corrosion-resistant tantalum metal. They are connected to sealed reservoirs by 10-cm-long capillaries to eliminate solvent evaporation and to provide an escape path for air bubbles formed during the filling process. The sample and reference cells are placed in an evacuated adiabatic chamber whose temperature is raised at a predetermined rate. The sample and refer-

ence cells are maintained at the same temperature as the adiabatic chamber. A 100-junction thermopile is used to sense the temperature difference between the sample and the reference cells and to provide a differential power signal to the sample needed to maintain it at the same temperature as the reference. This differential power is directly proportional to C_p , and is measured as a function of temperature. This calorimeter is capable of measuring small changes in specific heat by virtue of large sample mass and background compensation with a reference material. We obtained peak C_p values that were $\sim 20\%$ of the background. Although we lack the capabilities to perform cooling scans, they have been shown⁴ to be similar to the heating scans for this system.

Thermal equilibration is a concern for such large samples. We found that the results were independent of scan rate at rates slower than 50 mK/min. Thus, all of our scans were taken at heating rates between 11 and 37 mK/min. The temperature and specific-heat precisions of the calorimeter at these scan rates were ~ 7 mK and between 0.3% and 1.3%, respectively. We used densities

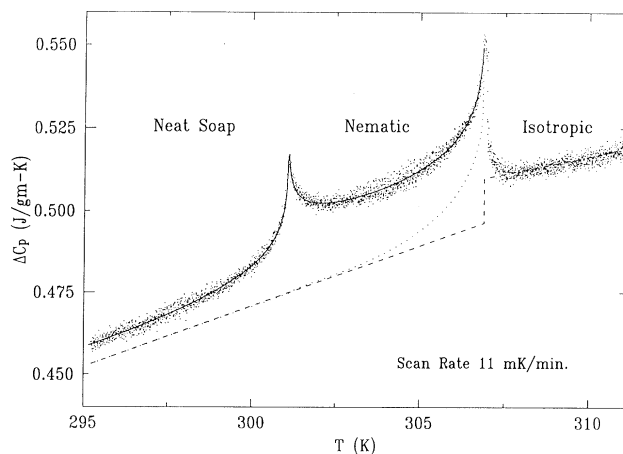


FIG. 1. ΔC_p vs temperature for the 2.7-mole%-CsPFO and water mixture. Solid line is a fit to the data as described in text. Dashed line is the background for the N-I transition.

TABLE I. Least-squares values of fitting parameters for the nematic-to-neat-soap transition in cesium-perfluoro-octanoate and water mixtures.

Conc. mole %	T_{N-NS} K	T_{N-I} K	A^+	A^+/A^-	α	D^+	D^-/D^+	C	α'	B	E	χ^2
2.24	293.480	299.517	0.096 ± 0.009	1.000	0.0005 ± 0.0002	0.003	-4.50	-3.18	-0.18	-172.95	-0.061	0.95
2.70	301.080	306.903	0.033 ± 0.002	1.001	0.0007 ± 0.0003	-0.004	6.71	15.08	0.005	-60.75	0.012	1.09
3.20	306.862	312.509	0.025 ± 0.003	1.003	0.0009 ± 0.0006	-0.025	1.74	27.59	0.003	-63.11	0.034	1.49
3.29	307.438	313.121	0.024 ± 0.001	1.003	0.0009 ± 0.0007	-0.101	1.01	33.72	0.002	-77.69	0.070	2.60
3.50	309.946	315.444	0.047 ± 0.006	1.001	0.0012 ± 0.0009	-0.010	7.65	19.97	0.006	-57.38	-0.001	1.30
3.70	312.418	317.820	0.055 ± 0.005	1.003	0.0031 ± 0.001	-0.011	12.34	13.65	0.007	-31.52	0.003	1.28
4.20	319.305	324.352	0.197 ± 0.023	1.012	0.012 ± 0.004	0.166	1.26	29.73	0.002	-73.27	0.090	0.91

as measured by Photinos and Saupe⁶ in our calculations of specific heat. Stirring the sample during measurements was considered unnecessary as the mixture is known⁴ to remain homogeneous for long periods of time. In fact, scans taken four months apart on the same sample were identical within experimental resolution, and without any discernible change in transition temperatures.

A representative scan, taken for a 2.7-mole% mixture over a 20-K range, is shown in Fig. 1. An increase in C_p due to pretransitional fluctuations on both sides of the N-NS transition is evident. The C_p peak height above background is ~ 0.06 J/gmK, which is in excellent agreement with the results of Ref. 4. The pretransitional effects below the N-I transition are more pronounced than above it. A finite coexistence region and jumps in specific heat are clearly visible, in Fig. 3, at this transition. Similar scans were obtained for the seven concentrations listed in Table I.

At the N-NS transition, the experimental data were fitted by the following expression:

$$C_p = (A^\pm/\alpha)t^{-\alpha}(1 + D^\pm t^{0.5}) + Ct'^{-\alpha'} + ET + B.$$

Here, A^\pm, D^\pm are the specific-heat amplitude and the coefficient of first correction-to-scaling term above (+) and below (-) the N-NS transition. $t = |T - T_{N-NS}|/T_{N-NS}$ and α is the specific-heat exponent. The second term represents the fluctuation specific heat near the N-I transition at the reduced temperature $t' = |T - T_c^*|/T_c^*$, T_c^* being the virtual second-order transition temperature, with exponent α' . The last two terms, with temperature T in K, provide a linear background. The constant B represents the sum of the regular and the critical back-

ground heat capacities. The fits without the correction-to-scaling term were not physically meaningful as they required different values of A and α above and below the transition. The solid line in Fig. 1 is a fit by the above function using all the data below the N-I transition. The

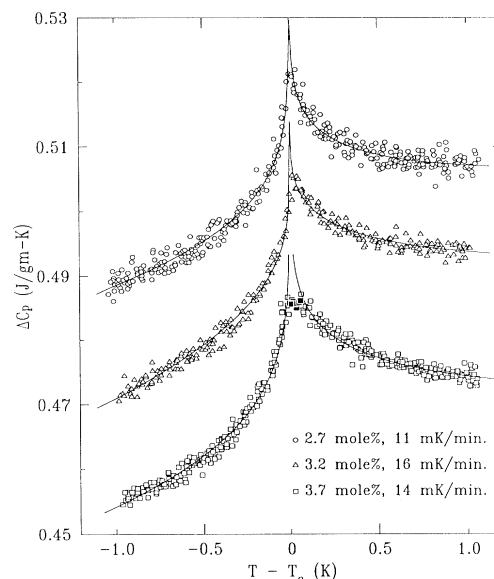


FIG. 2. ΔC_p vs $(T - T_c)$ for three samples within the ± 1 -K range of T_{N-NS} taken at the indicated scan rates. The solid lines are the best fits discussed in text. Solid squares are the data points in the coexistence region for the 3.7-mole% sample. The plots for 3.2 and 3.7 mole% have been shifted down for clarity by 0.018 and 0.034 J/gmK, respectively.

value of the parameters given in Table I remained within the errors when the data over a narrower range were used. Figure 2 shows such a fit obtained with points within ± 1 K of the transition. Similar results were obtained and are summarized in Table I for several other concentrations, three of which (2.7, 3.2, and 3.7 mole%) are shown in Fig. 2. The errors were determined by fixing α at values different from its best-fit value, and refitting the data to determine χ^2 . An F test was used to determine 95%-confidence limits on α .

The contribution to the background specific heat near T_{N-NS} due to the diverging specific heat at T_{N-I} was also approximated by a second-degree polynomial, instead of the power law ($t^{-\alpha}$) used above. Alternatively, a linear background in the NS phase was determined by drawing a tangent to the data far from T_{N-NS} , and subtracting it from the data. Then, only the divergent term with correction to scaling and a constant background term were used. We tried both of these fitting methods and several variations of them. The value of the critical exponents and the ratio of the specific-heat amplitudes, A^+/A^- , varied negligibly from those obtained with the first fit. Fits to the renormalization form of heat capacity obtained by replacing the first term in C_p by $A^\pm t^{-\alpha_R}/(1+B^\pm t^{-\alpha_R})$ did not give a stable α_R with the temperature range shrinking. The failure to fit the renormalization form of C_p and the small but positive value of α suggest that the renormalization is not occurring.

At 3.5-mole% concentration, the N and NS phases were found to coexist for ~ 21 mK. The coexistence region became even wider at higher concentrations: 77 and 351 mK for the 3.7- and 4.2-mole% mixtures, respectively. Experimental points in the coexistence region for the 3.7% mixture are shown as solid squares in Fig. 2. The quality of the fits obtained by excluding the points in the coexistence region were comparable to those for low-concentration mixtures, as seen for the 3.7-mole% mixture in Fig. 2. The value of α remained ~ 0 and did not approach the tricritical value of $\frac{1}{2}$. Discontinuous changes in C_p normally associated with the latent heat of a first-order transition are absent. Furthermore, the temperature range of the nematic phase in thermotropic materials becomes significantly narrower near a tricritical point. These effects are not observed up to the highest concentration of 4.2 mole%. We attribute the observed coexistence to impurity effects. Similar coexistence and rounding of transitions have been observed^{5,7,8} in the thermotropic materials 8OCB and 8CB. In our samples, high surfactant concentration is accompanied by a wider coexistence region as the tricritical point is approached. The source of impurities appears to be CsPFO, which, being an ionic compound, is likely to retain ionic contaminants in spite of the best efforts to purify it. The coexistence becomes so broad at higher concentrations that any meaningful estimates of α cannot possibly be made closer to the predicted¹ tricritical

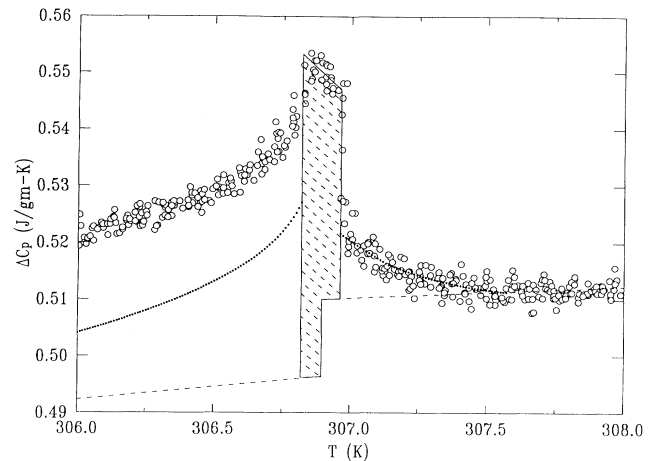


FIG. 3. ΔC_p near the N-I transition of 2.7 mole% shown on an expanded scale. The dashed line is the background used to calculate the transition enthalpy and the latent heat.

point.

The values of various parameters in our fits are summarized in Table I. The ratio of heat-capacity amplitudes remains almost unity as expected for 3D XY behavior. The values of α lie between 0.0005 and 0.012 with 40%–80% uncertainties. These values, although not exactly the same as predicted (~ -0.007) by the 3D XY model, are very close to it. Similar values of α (~ 0) have been reported for the thermotropic materials $\overline{6}O10+\overline{6}O8$,⁹ $\overline{8}S5$,¹⁰ and T7 and T8.¹⁰

The diverging part of the specific heat at T_{N-NS} was subtracted from the fits to obtain the background plus the specific heat associated with the pretransitional fluctuations at the N-I transition (see dotted line in Fig. 1). A tangent to this curve (dashed line) far from T_{N-I} provided the linear background below this transition. This background is joined with the background above the transition with a step change at T_{N-I} . The area under the specific heat (dotted) curve was used to determine the total enthalpy change which is equal to the sum of the latent heat ΔH and the integral of pretransitional specific heat, $\delta H (= \int \Delta C_p dT)$, at the N-I transition. The discontinuous changes in the specific heat above and below the N-I coexistence region, shown in Fig. 3 on an expanded scale, are due to the latent heat of transition. The latent heat of the N-I transition was calculated from the area under the C_p curve between the two discontinuities represented by the vertical lines. The N-I coexistence range is determined from the temperature difference between the onset of first discontinuity and the point at which the sharp drop in specific heat ends on the isotropic side of the peak. The latent heat and total enthalpy so obtained have an estimated accuracy of $\pm 5\%$.

A strong dependence of the latent heat and the coexistence range on concentration is evident in Fig. 4. The latent heat exhibits a quadratic dependence on molar

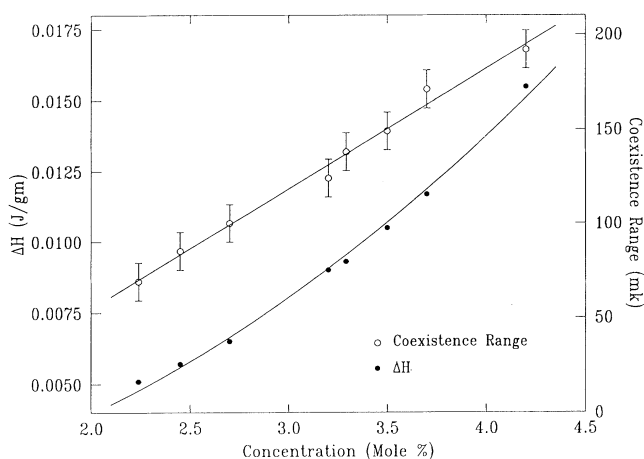


FIG. 4. Dependence of the N-I coexistence range and the latent heat (ΔH) on the molar concentration of CsPFO.

concentration of CsPFO, represented by the solid line. This is remarkably similar to the behavior of transition enthalpy near the nematic-smectic-*A* tricritical point⁸ in 9CB+10CB and 6O10+6O12 mixtures. It is consistent with the previous observation² of this transition becoming nearly second order at low concentrations. We extrapolate that this transition would become second order at ~ 1.2 mole% which, probably, lies below the Krafft temperature at which the solution freezes. The transition enthalpy remains nearly constant. This can be understood by noting that, as the transition becomes more and more nearly second order, it becomes possible to get closer to T_c^* and detect a larger contribution from more pronounced pretransitional fluctuations. Thus, any decrease in the latent heat is compensated by an increase in the fluctuation specific heat.

To summarize, we have reported the measurements and the first quantitative analysis of the specific heat at the N-NS and N-I phase transitions in a lyotropic liquid crystal. The specific-heat amplitude ratio and value of α at the N-NS transition suggest 3D XY-type behavior. A

decrease in the latent heat and coexistence range with decreasing concentration observed at the N-I transition suggest an approach to a Landau point.

We thank Professor D. L. Johnson, Professor C. W. Garland, Professor J. Thoen, and Dr. G. Nounesis for enlightening discussions and helpful suggestions for data analysis. The surfactant CsPFO was synthesized by Dr. M. Neubert and S. Keast under NSF Grant No. DMR-88-18561. The computing resources for the data analysis were provided by the Ohio Supercomputer Center. This work was supported by the National Science Foundation Grant No. DMR-88-19680.

¹N. Boden, P. H. Jackson, K. McMullen, and M. C. Holmes, Chem. Phys. Lett. **67**, 476 (1979); N. Boden and M. C. Holmes, Chem. Phys. Lett. **109**, 76 (1984); N. Boden, K. W. Jolley, and M. H. Smith, Liq. Cryst. **6**, 481 (1989).

²S. Kumar, J. D. Brock, M. Sutton, and J. D. Litster, in *Surfactant in Solutions*, edited by K. L. Mittal (Plenum, New York, 1989), Vol. 8, p. 35, and references therein.

³S. Kumar, L. J. Yu, and J. D. Litster, Phys. Rev. Lett. **50**, 1672 (1983).

⁴S. Imaizumi and C. W. Garland, J. Phys. Soc. Jpn. **58**, 597 (1989).

⁵D. L. Johnson, C. F. Hayes, R. J. deHoff, and C. A. Schantz, Phys. Rev. B **18**, 4902 (1978).

⁶P. Photinos and A. Saupe, J. Chem. Phys. **90**, 5011 (1989).

⁷G. B. Kasting, C. W. Garland, and K. J. Lushington, J. Phys. (Paris) **41**, 879 (1980).

⁸G. B. Kasting, K. J. Lushington, and C. W. Garland, Phys. Rev. B **22**, 321 (1980); J. Thoen, H. Marynissen, and W. Van Dael, Phys. Rev. A **26**, 2886 (1982).

⁹J. Thoen, H. Marynissen, and W. Van Dael, Phys. Rev. Lett. **52**, 204 (1984); M. A. Anisimov, Mol. Cryst. Liq. Cryst. **162A**, 1 (1988), and references therein.

¹⁰D. Brisbin, R. DeHoff, T. E. Lockhart, and D. L. Johnson, Phys. Rev. Lett. **43**, 1171 (1979); K. W. Evans-Lutterodt, J. W. Chung, B. M. Ocko, R. J. Birgeneau, C. Chiang, C. W. Garland, E. Chin, J. Goodby, and N. H. Tinh, Phys. Rev. A **36**, 1387 (1987).